Supporting Information

Bai et al. 10.1073/pnas.1708744114

SI Materials and Methods

Materials. CL316243, amlexanox, dideoxycytidine (ddC), carbonyl cyanide-4-(trifluoromethoxy) phenylhydrazone (FCCP), rotenone, antimycin A, D-(+)-glucose, insulin, zardaverine, H-89, and 3′-isobutyl-1-methylxanthone were from Sigma; L-glutamine and pyruvate were from Gibco; oligomycin was from Calbiochem; 2′3′-cGAMP and 2′3′-cGAMP control were from InvivoGen; ABT-737 and nigericin were from Cayman Chemical; ethidium bromide (EtBr) was from Bio-Rad; digitonin was from EMD Millipore; and insulin (Humulin R) used for insulin tolerance testing was from Eli Lilly. Anti-PE MicroBeads were from Miltenyi Biotec; antibody to cGAS was from EMD Millipore; antibody to ERp57 was obtained from Abcam; antibody to Complex IV was from Molecular Probes; lamin A antibody was from BioVision; TNF-α antibody was from Cell Applications; PE-conjugated F4/80 antibody was from BioLegend; adiponectin and DsbA-L antibodies were homemade from rabbit; and antibodies to beta-tubulin and myc were made from monoclonal antibody-producing cell lines obtained from ATCC. All other antibodies were from Cell Signaling.

Detection of mtDNA Content in Cytosolic Extracts. Cytosolic mtDNA content was measured according to the procedure described (4). Cultured adipocytes (8.8×10^6) or freshly purified mouse adipocytes were each divided into two aliquots of equal volume. One aliquot was resuspended in 500 μL DNA extraction buffer (100 mM Tris·HCl, pH 8.5, 5 mM EDTA, pH 8.0, 0.2% SDS, 200 mM NaCl, 100 μg/mL proteinase K) to extract total DNA, which served as normalization controls for total mtDNA. The second aliquot was resuspended in 500 μL buffer containing 150 mM NaCl, 50 mM Hepes (pH 7.4), and 25 μg/mL digitonin. The homogenates were incubated end-over-end for 10 min to allow for selective plasma membrane permeabilization and then centrifuged three times at $980 \times g$ for 5 min to pellet intact cells. The first pellet was saved as the "Pel" fraction for Western blotting. The cytosolic supernatants were transferred to fresh tubes and spun at $17{,}000 \times g$ for 25 min to pellet any remaining cellular debris, yielding cytosolic preparations free of nuclear, mitochondrial, and endoplasmic reticulum contamination. DNA was then isolated from these pure cytosolic fractions using QIAquick Nucleotide Removal Columns (Qiagen). Quantitative PCR was performed on both whole-cell extracts and cytosolic fractions using nuclear DNA primers (Tert) and mtDNA primers (Dloop1 to 3, mtND4, and Cytb), and the cycle threshold (CT) values obtained for mtDNA abundance for whole-cell extracts served as normalization controls for the mtDNA values obtained from the cytosolic fractions. This allowed for effective standardization among samples and controlled for any variations in the total amount of mtDNA in samples. Using this digitonin method, no nuclear Tert DNA was detected in the cytosolic fractions, indicating nuclear lysis did not occur.

F4/80+ Adipose Tissue Macrophage Isolation. The F4/80+ adipose tissue macrophage (MΦ) fraction was purified from the SVF by anti-PE MicroBead-based magnetic separation as described by the manufacturer's instructions. Briefly, a total of 10^7 SVF cells was resuspended in 100 μL PBS buffer and stained with 10 μL PE-conjugated F4/80 antibody for 10 min at 4 °C. Cells were washed and then incubated with 20 μL anti-PE MicroBeads for 15 min. Washed cells were resuspended in 1 mL PBS buffer and applied to LS columns (MACS Miltenyl Biotec). The MΦ-positive and SVF-MΦ−negative (SVF-MΦ-Neg) cells were eluted and collected for further analysis. The percentages of MΦ and SVF-MΦ-Neg cells were analyzed on a BD FACSCanto II Cytometer (BD Biosciences) with FlowJo software.

Body Weight and Composition. Mouse body weight and food intake were measured on a weekly basis. Bone mineral density, fat mass, lean mass, and percentage of fat were determined using dual-energy X-ray absorptiometry (DEXA) (GE Medical Systems).

Glucose and Insulin Tolerance Tests. Six-week-old male DsbA-L^{fKO} and control mice were fed a normal chow or high-fat diet (45% kcal from fat; D12451; Research Diets) for 12 wk. Glucose and insulin tolerance tests were performed as described in our previous study (42).

Hematoxylin and Eosin Staining. For H&E staining, adipose and liver tissues were first fixed in 10% formalin for 20 h and embedded in paraffin. Five sections (10 μm thick) per animal were cut at positions distributed equally throughout the fat pad and three pictures were obtained per section. Tissue sections were then stained with H&E.

Fat Cell Size and Number Measurement. Fat cell size and number measurement were performed according to the procedure described (42). The average adipocyte cell diameter was analyzed using NIH ImageJ software. Total adipocyte numbers were estimated by manually counting cells on H&E slides from at least three 20× fields per mouse. Cell size was approximated assuming cubic packing as described (42).

Determination of Adiponectin Multimers. Size-exclusion chromatography studies were performed as described in our previous study (23). The distribution of adiponectin multimers was determined by gel filtration fast-protein liquid chromatography using a Superdex 200 column (GE Healthcare Life Sciences); 200-μL fractions were collected and separated by SDS/PAGE, followed by Western blot analysis.

ROS Detection. Mitochondria from adipocytes were isolated according to a published protocol (43). For dichlorofluorescein diacetate-based ROS measurement, isolated mitochondria or whole cells were incubated in assay buffer [5 mM pyruvate and malate, 2 mM ADP, 100 mM KCl, 2 mM $MgCl_2$, 1 mM EDTA, 4 mM KH_2PO_4, 20 mM Tris-EDTA-SDS (TES), pH 7.4] with the ROS detection reagent 2′,7′-dichlorodihydrofluorescein diacetate. Hydrogen peroxide-releasing kinetics were detected at excitation (Ex)493/emission (Em)527 using a fluorescence microplate reader.

ATP Levels. ATP levels were measured by a chemiluminescence assay with an ATP determination kit (Thermo Fisher Scientific) following the manufacturer's instructions. To determine the ATP production rate in adipocytes, aliquots of freshly isolated mitochondria were incubated with a luciferin-luciferase ATP-monitoring reagent in the reaction buffer. The reactions were performed in an opaque 96-well plate, and the luciferase signal was detected at 560 nm using a Synergy HT Multi-Detection Microplate Reader (BioTek Instruments).

Measurement of Membrane Potential. Mitochondrial membrane potential was measured based on the protocol described (44). Cells were incubated with 200 nM tetramethylrhodamine, methyl ester (TMRM; Thermo Fisher Scientific) and 10 ng/mL nuclear staining dye Hoechst-33342 (Invitrogen) in a 37 °C, 5% CO_2

incubator for 20 min. Next, 10 cells were collected and transferred to an opaque, black 96-well microplate. Fluorescence was recorded for TMRM at Ex540/Em575 and Hoechst-33342 at Ex350/Em461 using a Synergy HT Multi-Detection Microplate Reader. TMRM fluorescence was normalized to the Hoechst reading.

NAD^+/NADH Ratio. The NAD^+/NADH ratio was determined by a fluorescence NAD/NADH detection kit (Cell Technology). Adipocytes (6×10^6) were divided into two aliquots of equal volume and incubated with either NAD or NADH extraction buffer; 200 μL of the NAD/NADH lysis buffer was used to homogenize the samples. The samples were then gently vortexed and heated at 60 °C for 15 min. Reaction buffer and the opposite extraction buffer were added to neutralize the samples, which oxidize NADH to its fluorescent analog and NAD, the latter of which is further converted to NADH via an enzyme-coupled reaction. The fluorescence signal was detected at Ex540/Em590.

Seahorse Oxygen Consumption Assay. Oxygen consumption rates (OCRs) were measured in primary culture adipocytes using a Seahorse Bioscience XFe96 Analyzer. In brief, 5,000 cells were plated per well in 0.2% (wt/vol) gelatin-coated 96-well Seahorse XF cell-culture plates. After 2 d of growth, the cells reached confluence and were differentiated as described (23). The cellular OCR was analyzed in Seahorse XF assay medium supplemented with 25 mM glucose, 1 mM pyruvate, and 2 mM glutamine with the following inhibitors: 2 μM oligomycin, 5 μM FCCP, 2 μM rotenone, and 2 μM antimycin A.

2′3′-cGAMP Analysis by HPLC-Electrospray Ionization Tandem Mass Spectrometry. Five million cells were extracted using cold 80% MeOH and 2% acetic acid and placed at −80 °C for 1 h. The extract was dried down and reconstituted in 50 μL of deionized water suitable for HPLC-electrospray ionization tandem mass spectrometry analysis. LC-MS analyses were performed in positive electrospray mode on a Thermo Fisher Q Exactive with online separation and with a Thermo Fisher/Dionex UltiMate 3000 HPLC system. The conditions used for 2′3′-cGAMP analyses were: column, Kinetex C18, 2.6 μm, 2.1 × 100 mm (Phenomenex); mobile phase A, 0.1% acetic acid with 10 mM ammonium acetate in water; mobile phase B, methanol; flow rate, 250 μL/min; gradient, held at 1% B for 5 min and run from 1% B to 30% B over 4 min. Full-scan mass spectra were acquired on the Orbitrap over an m/z range of 100 to 1,000 at 70,000 resolution (m/z 300). Metabolite identification was based on the metabolite accurate mass (±5 ppm) and was in agreement with the HPLC retention time of authentic standards. Quantification was made by integration of extracted ion chromatograms followed by comparison with the corresponding standard curves.

Generation of cGAS and STING shRNA Plasmids. The sense and antisense sequences for shRNA constructs were chemically synthesized and ligated into the pRNATin-H1.2/Adeno vector (GenScript). The sense strand sequences were m-cGAS: 5′-GTGAGGACCAATCTAAGAC-3′ and m-STING: 5′-GAGCTTGACTCCAGCGGAA-3′ (45).

Analysis of Cytokine and Chemokine Production. The serum cytokines and chemokines were measured using a Mouse Procarta-Plex Cytokine & Chemokine Panel 1 (26-plex) Multiplex Immunoassay Kit (Thermo Fisher Scientific). Briefly, 25 μL of serum samples was incubated with antibody-coupled beads at 4 °C overnight. Complexes were washed and then incubated with a biotinylated detection antibody for 30 min. Streptavidin-phycoerythrin was added and incubated for another 30 min before assessing cytokine and chemokine concentrations. Fourfold serial dilutions of the recombinant cytokines or chemokines provided by the vendor were used to establish standard curves. Cytokine and chemokine levels were determined using a Flexmap 3D System (Luminex) at the BASiC Core at UTHSA. The concentration was calculated using software provided by the manufacturer (Bio-Plex Manager software).

Real-Time qPCR. Tissue samples were homogenized in TRIzol (Invitrogen), and total RNA was isolated according to the manufacturer's suggested protocol; 1 μg of RNA was used for cDNA synthesis (Qiagen). Quantitative PCR reactions were performed using SYBR Green (Applied Biosystems) and quantitated using an Applied Biosystems 7900 HT sequence detection system. Duplicate runs of each sample were normalized to β-actin to determine relative expression levels. A complete list of primers and sequences is in Table S1.

Statistics. For cell studies, data are representative of three independent experiments. The Western blot images were semi-quantified with the NIH Scion Image program. Statistical analysis of the data was performed using GraphPad Prism 6. Significance was assessed by performing an unpaired two-tailed Student's t test as indicated in individual figures. No statistical method was used to predetermine sample size. Quantitative data are presented as mean ± SEM. Statistical significance was set at $^*P < 0.05$, $^{**}P < 0.01$, $^{***}P < 0.001$.

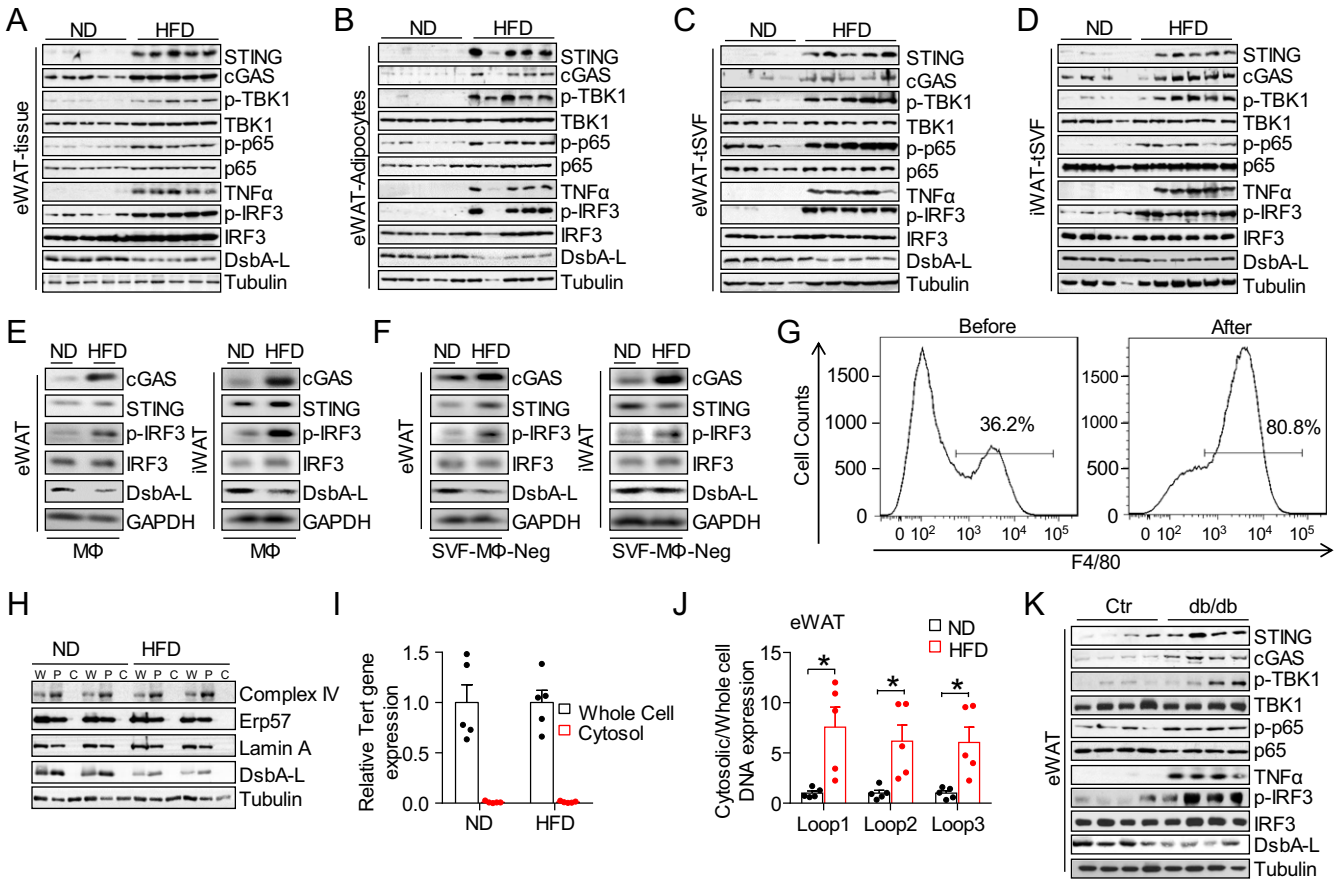

Fig. S1. cGAS-cGAMP-STING pathway was activated in adipose tissues from obese mice. (*A*) Immunoblot analysis of eWAT from a normal chow diet (ND)- and high-fat diet (HFD)-fed C57BL/6 mice. (*B*) Immunoblot analysis of purified adipocytes from eWAT of ND- and HFD-fed C57BL/6 mice. (*C* and *D*) Immunoblot analysis of total SVF (tSVF) from (*C*) eWAT and (*D*) iWAT of ND- and HFD-fed C57BL/6 mice. (*E* and *F*) Immunoblot analysis of (*E*) adipose-resident F4/80+ macrophage and (*F*) macrophage-negative SVF fractions (SVF-MΦ-Neg) from ND- and HFD-fed C57BL/6 mice; each blot represents the average level of 10 mice. (*G*) Percentage of macrophages from adipose-tissue SVF before or after magnetic separation shown by FACS analysis. (*H*) Purified adipocytes from ND- and HFD-fed mice were subjected to digitonin fractionation as described in *SI Materials and Methods*, and whole-cell extracts (W), pellets (P), and cytosolic extracts (C) were detected by immunoblot using the indicated antibodies. (*I*) Nuclear-encoded Tert gene expression was quantitated via qPCR in whole-cell and cytosolic extracts from freshly purified adipocytes of ND- and HFD-fed mice. (*J*) Cytosolic mtDNA content in freshly purified adipocytes from eWAT of ND- and HFD-fed C57BL/6 mice, $n = 5$. (*K*) Immunoblot analysis of eWAT from db/db mice and their control mice. Data are presented as mean ± SEM. $^*P < 0.05$.

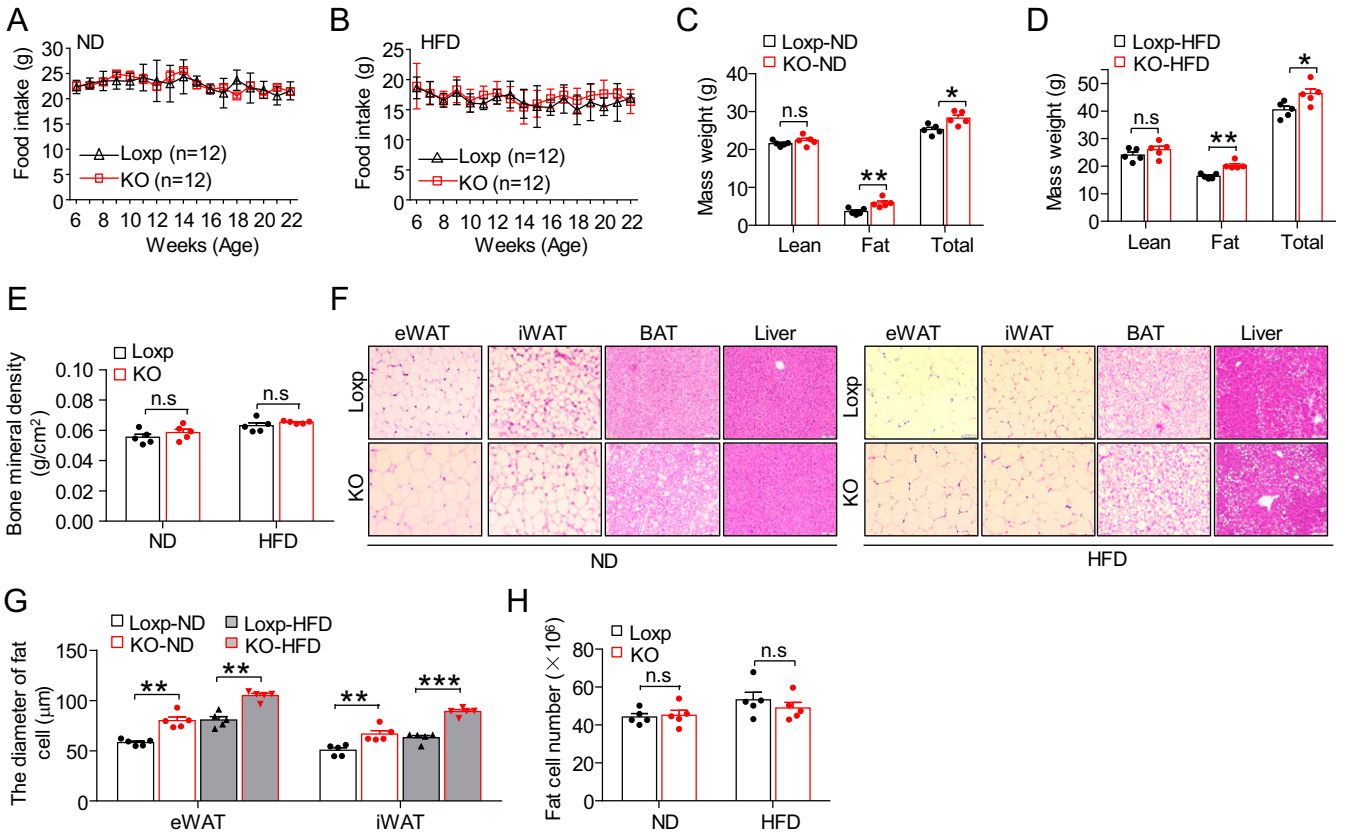

Fig. S2. Fat-specific disruption of DsbA-L leads to fat expansion in mice. (*A* and *B*) Food intake of DsbA-L^{fKO} and Loxp control mice during (*A*) ND feeding or (*B*) HFD feeding. (*C* and *D*) Tissue composition of 4-mo-old DsbA-L^{fKO} and Loxp control mice fed (*C*) ND or (*D*) HFD as determined by DEXA. (*E*) Bone mineral density of 4-mo-old DsbA-L^{fKO} and Loxp control mice fed ND or HFD as determined by DEXA. (*F*) A representative H&E stain of eWAT, iWAT, BAT, and liver from DsbA-L^{fKO} and Loxp control mice fed ND or HFD. (Scale bars, 50 μm.) (*G*) The average diameters of fat cells in DsbA-L^{fKO} and Loxp control mice fed ND or HFD were analyzed and quantified by NIH ImageJ software. (*H*) Numbers of fat cells in DsbA-L^{fKO} and Loxp control mice fed ND or HFD. Data are presented as mean ± SEM. **P* < 0.05, ***P* < 0.01, ****P* < 0.001. n.s, not significant.

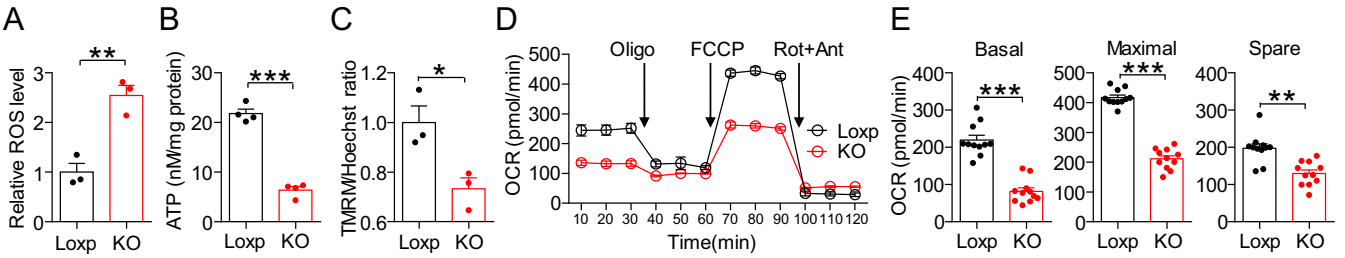

Fig. S3. DsbA-L deficiency impairs mitochondrial function in adipocytes. (*A*) Mitochondrial reactive oxygen species, (*B*) ATP levels, (*C*) membrane potential, and (*D* and *E*) oxygen consumption rate were determined in primary adipocytes of DsbA-L^{fKO} and Loxp control mice. Data are presented as mean ± SEM. **P* < 0.05, ***P* < 0.01, ****P* < 0.001.

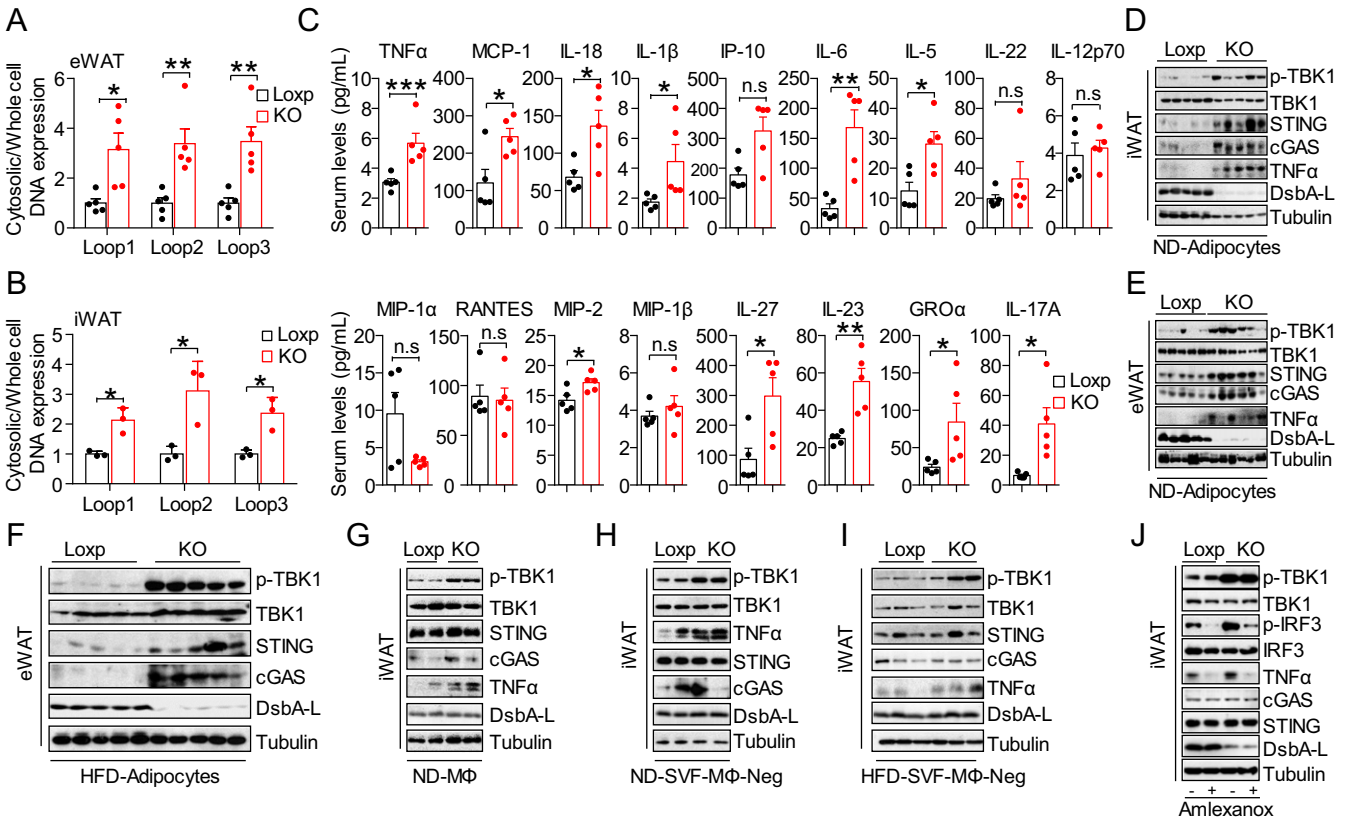

Fig. S4. DsbA-L deficiency in adipocytes induces mtDNA release and inflammation. (*A* and *B*) Cytosolic mtDNA content in freshly purified adipocytes from (*A*) eWAT or (*B*) primary cultured iWAT of DsbA-L^{fKO} and Loxp control mice. (*C*) Serum levels of cytokines and chemokines from DsbA-L^{fKO} and Loxp control mice. (*D–F*) Immunoblot analysis of purified adipocytes from DsbA-L^{fKO} and Loxp control mice fed (*D* and *E*) ND or (*F*) HFD. (*G*) Immunoblot analysis of F4/80+ macrophages from DsbA-L^{fKO} and Loxp control mice fed ND; each blot represents the average level of five mice. (*H* and *I*) Immunoblot analysis of adipose-resident macrophage-negative SVF fractions (SVF-MΦ-Neg) from DsbA-L^{fKO} and Loxp control mice fed (*H*) ND or (*I*) HFD. (*J*) Immunoblot analysis of primary inguinal adipocytes from DsbA-L^{fKO} and Loxp control mice treated with or without 50 μM amlexanox for 12 h. Data are presented as mean ± SEM. $*P < 0.05$, $**P < 0.01$, $***P < 0.001$. n.s, not significant.

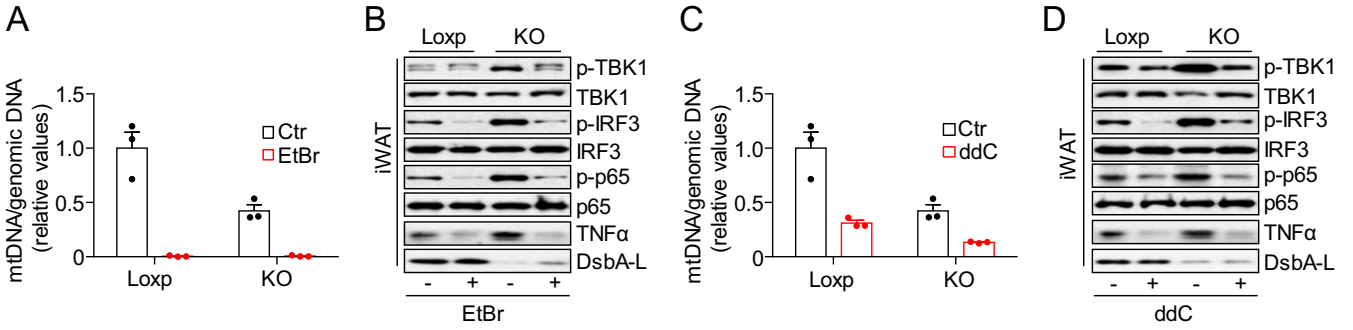

Fig. S5. mtDNA depletion diminished activation of the cGAS-cGAMP-STING pathway. (*A* and *C*) Total mtDNA content was quantitated via qPCR using nuclear DNA primers (Tert) and mtDNA primers (mtND1) in primary iWAT treated with or without (*A*) 0.25 μg/mL EtBr and (*C*) 100 μM ddC for 3 d. (*B* and *D*) Immunoblot analysis of primary inguinal adipocytes treated with or without (*B*) EtBr and (*D*) ddC for 3 d. Data are presented as mean ± SEM.

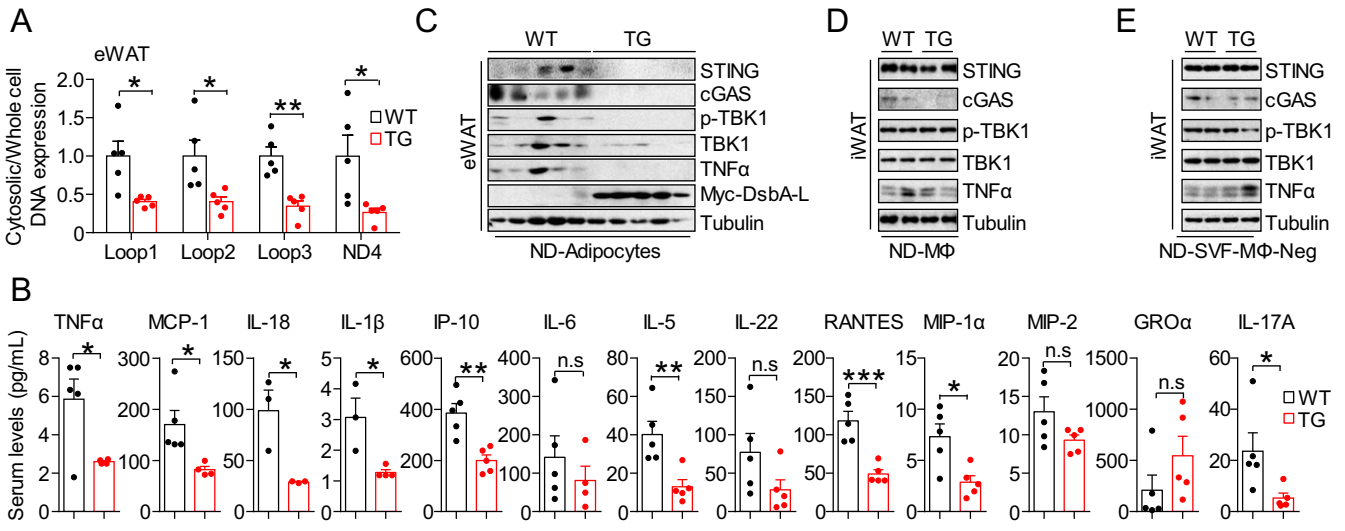

Fig. S6. Overexpression of DsbA-L protects against HFD-induced mtDNA release and inflammation. (*A*) Cytosolic mtDNA content in freshly purified adipocytes from eWAT of DsbA-L^{fTG} mice and wild-type control mice fed HFD. (*B*) Serum levels of cytokines and chemokines from HFD-fed DsbA-L^{fTG} and wild-type control mice. (*C*–*E*) Immunoblot analysis of (*C*) purified adipocytes, (*D*) MΦ, and (*E*) SVF-MΦ-Neg fractions from DsbA-L^{fTG} and control mice fed ND. Data are presented as mean ± SEM. $*P < 0.05$, $**P < 0.01$, $***P < 0.001$. n.s, not significant.

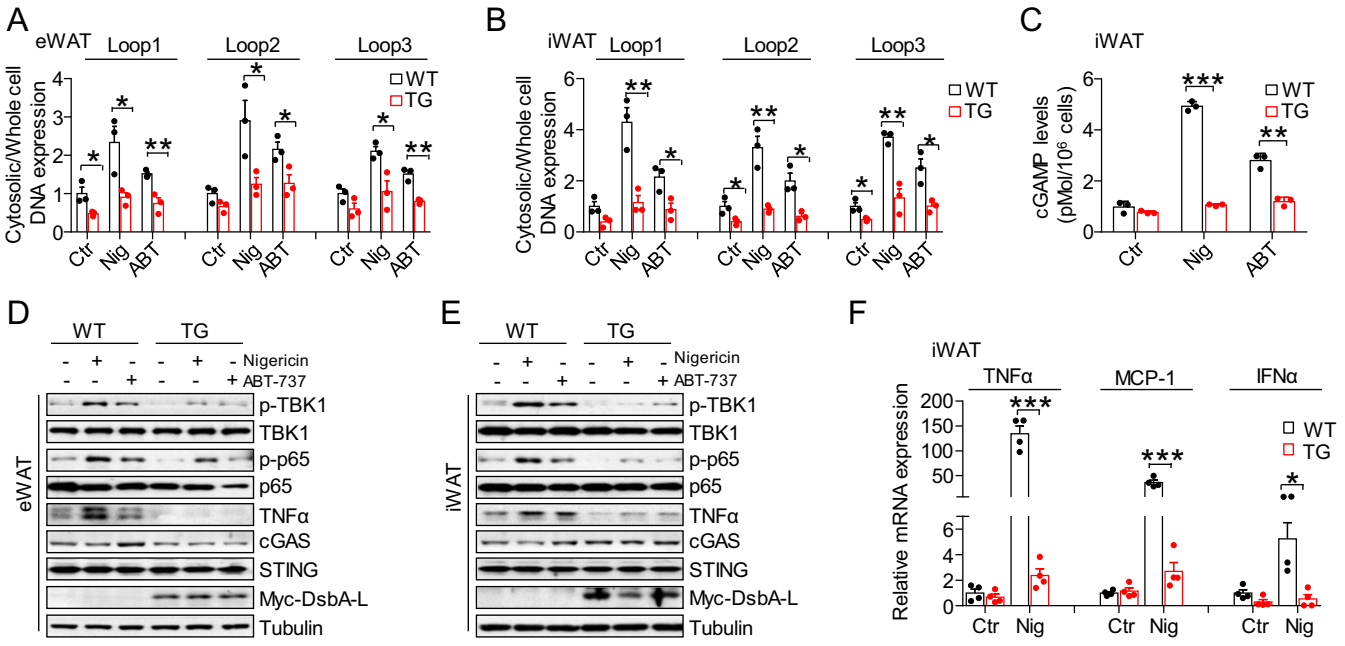

Fig. S7. Overexpression of DsbA-L alleviates chemical-induced mtDNA release and inflammation. (*A* and *B*) Cytosolic mtDNA content, (*C*) 2′3′-cGAMP levels, (*D* and *E*) immunoblot analysis, and (*F*) inflammatory gene mRNA levels in primary adipocytes treated with or without 4 μM nigericin or 10 μM ABT-737 for 12 h. Data are presented as mean ± SEM. $*P < 0.05$, $**P < 0.01$, $***P < 0.001$.

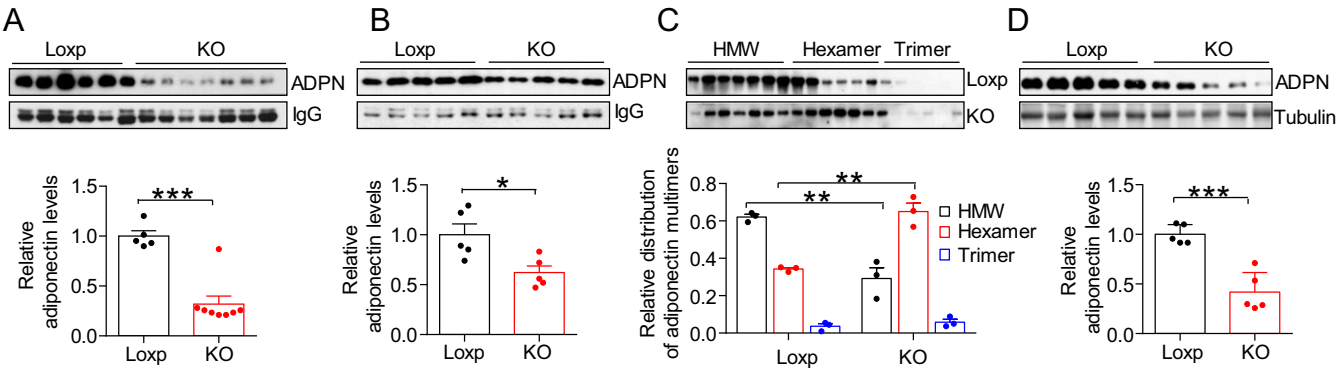

Fig. S8. Adiponectin levels and multimerization are reduced in DsbA-L–deficient mice. (*A* and *B*) Immunoblot analysis of serum adiponectin (ADPN) levels from DsbA-L^{fKO} and Loxp control mice fed (*A*) ND or (*B*) HFD. (*C*) Serum adiponectin multimers from DsbA-L^{fKO} and Loxp control mice fed ND were separated by FPLC and immunoblotted with an antibody to adiponectin. HMW, high molecular weight. (*D*) Immunoblot analysis of adiponectin expression in eWAT from DsbA-L^{fKO} and Loxp control mice fed ND. Data are presented as mean ± SEM. $*P < 0.05$, $**P < 0.01$, $***P < 0.001$.

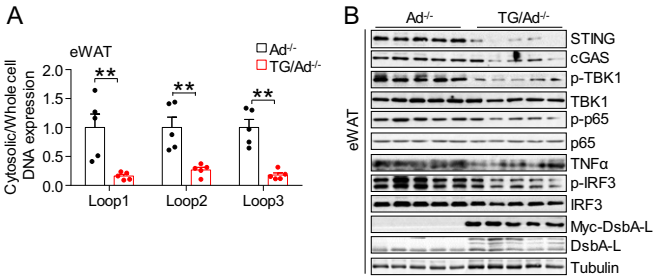

Fig. S9. DsbA-L protects against HFD-induced mtDNA release through an adiponectin-independent mechanism. (*A*) Cytosolic mtDNA content in freshly purified adipocytes from eWAT of Ad$^{-/-}$ mice and DsbA-L^{fTG}/Ad$^{-/-}$ mice fed HFD. (*B*) Immunoblot analysis of eWAT from Ad$^{-/-}$ mice and DsbA-L^{fTG}/Ad$^{-/-}$ mice fed HFD. Data are presented as mean ± SEM. $**P < 0.01$.

Table S1. Primer pair sequences

Gene	Accession no.	Primer	Sequence, 5′-3′
DsbA-L	NM_029555.2	Forward	ATGGATGCGTGTATGGTCTC
		Reverse	CAACAGTGGTGGGTAGCG
β-Actin	NM_007393.5	Forward	GTTGGTTGGAGCAAACATC
		Reverse	CTTATTTCATGGATACTTGGAATG
TNF-α	NM_013693.3	Forward	GAGAAAGTCAACCTCCTCTCTG
		Reverse	GAAGACTCCTCCCAGGTATATG
MCP-1	NM_011333.3	Forward	CAGCCAGATGCAGTTAACGC
		Reverse	GCCTACTCATTGGGATCATCTTG
IFN-α	NM_010502.2	Forward	CCTGCTCTCTAGGATGTG
		Reverse	TTTGTACCAGGAGTGTCA
IL-18	XM_017313137.1	Forward	TCTTGGCCCAGGAACAATGG
		Reverse	ACAGTGAAGTCGGCCAAAGT
mtDNA loop 1	NC_005089	Forward	AATCTACCATCCTCCGTGAAACC*
		Reverse	TCAGTTTAGCTACCCCCAAGTTTAA
mtDNA loop 2	NC_005089	Forward	CCCTTCCCCATTTGGTCT*
		Reverse	TGGTTTCACGGAGGATGG
mtDNA loop 3	NC_005089	Forward	TCCTCCGTGAAACCAACAA*
		Reverse	AGCGAGAAGAGGGGCATT
mtND4	NC_005089	Forward	AACGGATCCACAGCCGTA*
		Reverse	AGTCCTTCGGGCCATGATT
Tert	NC_000079.6	Forward	CTAGCTCATGTGTCAAGACCCTCTT*
		Reverse	GCCAGCACGTTTCTCTCGTT

*From ref. 4.